Near Surface Geophysics EAGE

Near Surface Geophysics, 2022, **20**, 82–93 doi: 10.1002/nsg.12183

Diagnostics of asphalt pavement using elastic standing waves

L. Ngomayezwe[1]*, Yu. I. Kolesnikov[2,3,4] and K. V. Fedin[2,4]

[1]*Scientific and Industrial Research and Development Centre, Harare, Zimbabwe,* [2]*Trofimuk Institute of Petroleum Geology and Geophysics, SB RAS, Novosibirsk, Russia,* [3]*Seismological Branch of Unified Geophysical Service, RAS, Novosibirsk, Russia, and* [4]*Novosibirsk State University, Novosibirsk, Russia*

Received October 2020, revision accepted November 2021

ABSTRACT

To ensure the safe operation of roads, it is necessary to periodically monitor the condition of road surfaces. Lately, near-surface geophysics methods have been actively used to solve such problems. The seismoacoustic methods that are used to diagnose road surfaces are typically dynamic methods based on the excitation of body or surface elastic waves in the road surfaces. The purpose of this work is to assess the possibilities of using elastic standing waves for diagnosing a hard road surface. This article presents the results of field experiments that demonstrate the possibility of detecting cavities under an asphalt pavement using flexural standing waves. Such waves, like vibrations of a membrane fixed or partially fixed at its edges, can be formed on the hard surface cover above the cavity as a result of exposure to acoustic noise. In this article, the accumulation of amplitude spectra of a large number of noise records was used to extract standing waves from the acoustic noise recorded on the surface of the pavement. It is shown that the joint visualization of the averaged spectra obtained by profile observations over the cavity makes it possible to confidently identify several modes of flexural standing waves. Based on the areal measurements, a map of the distribution of the amplitudes of one of the modes of flexural standing waves in the asphalt pavement over the cavity was constructed. At a qualitative level, this distribution is consistent with the results of computer simulations using the finite element method. The fact that, under the influence of acoustic noise in the pavement, the flexural standing waves are formed which are absent at other places indicates the absence of rigid contact at its lower boundary. Thus, the horizontal dimensions of the cavity can be estimated from the size of the area on which flexural standing waves are formed. In addition, the article shows that the analysis of vertical compressional (but not flexural) standing waves arising in the pavement under the influence of noise allows us to investigate the thickness of the pavement and to qualitatively assess the ratio of acoustic stiffness of the pavement and the underlying layer.

Key words: Finite-element, Geophone, Modelling, Sinkhole, Waves.

INTRODUCTION

To ensure the safe operation of roads, it is necessary to periodically monitor the condition of road surfaces. Such monitoring may be carried out by various methods, such as visual inspection, drilling with selection and consequent drill sample analysis, and measurement of deflection with deflectometers, etc.

Lately, near-surface geophysical methods are increasingly being used to study the quality and condition of pavements.

*Email: Lngomayezwe@gmail.com

Typically, to solve such problems, ground-penetrating radar technologies are used (Saarenketo and Scullion, 2000; Derobert *et al*., 2001; Kulizhnikov, 2001; Al-Qadi *et al*., 2003; Al-Qadi and Lahouar, 2005, Benedetto and Pensa, 2007; Cassidy *et al*., 2011; Li *et al*., 2015, 2016; Kassem *et al*., 2016; Fedorova *et al*., 2017; Khamzin *et al*., 2017), but other geophysical methods have also been used to investigate the condition of pavements, for example electro-tomography (Olenchenko and Kondrat'ev, 2017) and capacitance methods (Dashevsky *et al*., 2005).

Seismoacoustic methods are also widely used to diagnose road surfaces. Typically, these methods are based on the analysis of surface (Nazarian *et al*., 1993; Baker *et al*., 1995; Celaya and Nazarian, 2006; Li *et al*., 2016; Iodice *et al*., 2019) or body (Nazarian *et al*., 1993; Baker *et al*., 1995; Khazanovich *et al*., 2005; Cassidy *et al*., 2011; Hoegh *et al*., 2011; Hoegh *et al*., 2012; Li *et al*., 2016; Freeseman *et al*., 2018; Choi and Park, 2019; Salles *et al*., 2019) waves, which are excited at the surface with the help of various dynamic sources (shocks, vibrators, etc). In addition, passive seismoacoustic methods based on the analysis of vibrations that occur at the road surface from uncontrolled sources, such as vehicles, running crowds, seismic activity, etc., have recently been developed. This approach, for example, is implemented in a multifunctional system for the management of structures and infrastructures (Merenda *et al*., 2019), where spectral analysis, the wavelet transform of noise signals and neural networks are used to assess the condition of the road surface.

Despite the variety of pavement inspection methods and the tasks that they solve, the accuracy and authenticity of the results do not always comply with requirements. For example, widely used ground-penetrating radar technologies or pulse seismoacoustic methods can surely highlight contrast inhomogeneities under the pavement, but they are not always able to determine the type of inhomogeneities. For example, distinguishing a cavity in the pavement from other inhomogeneities.

At the same time, one of the topical problems of road diagnostics is related to cavity formation below road's asphalt–concrete coating. Such cavities may develop due to base level erosion under the pavement and seasonal variations, which are caused by frost heave and defrost subsidence, etc. The identification of such voids is particularly difficult because it is visually impossible to determine them at the initial stage, but under certain conditions (an increase in its dimensions, traffic load, etc.) they may lead to instantaneous destruction of asphalt pavement, which may lead to an emergency situation.

The purpose of this work is to assess the possibility of using elastic standing waves to diagnose a hard road surface. The results presented in this article demonstrate the effectiveness of elastic standing waves in detecting and delineating cavities under an asphalt pavement, to investigate its thickness and to estimate qualitatively the ratio of the acoustic stiffness (product of longitudinal wave velocity by density) of the pavement to the underlying layer.

JUSTIFICATION OF USING ELASTIC STANDING WAVES FOR THE DIAGNOSIS OF ASPHALT PAVEMENTS

Introductory notes

It is known that a standing wave is produced as a result of the interference of two harmonic waves with the same frequencies and amplitudes propagating towards each other (Khaykin, 1971; Pain, 2005). In a standing wave, vibrations are not transmitted from point to point, that is it does not transfer energy in space. A typical example of such waves is the vibration of a string fixed at both ends (the fundamental tone and overtones). If the amplitudes of the interfering travelling waves and/or the directions of their propagation differ, then as a result of the interference both a standing wave and a new travelling wave are formed.

In confined objects, standing waves can arise due to the interference of internal reflections of travelling waves from various sources, including noise sources, and the spectra of which contain frequency components corresponding to the natural frequencies of these objects. The energy generated by noise sources of standing waves can only represent a relatively small fraction of the total energy of the wave field. However, as shown by physical modelling and field experiments (Kolesnikov and Fedin, 2018; Kolesnikov *et al*., 2019; Fedin *et al*., 2021), the accumulation of amplitude spectra of a large number of noise records allows one to confidently determine the frequencies of standing waves generated in the object under study. These frequencies can be used to assess the properties and state of an object.

On a hard road surface, standing waves can be formed by the interference of various types of waves – body (compressional and shear), Lamb (symmetric and anti-symmetric), surface (Rayleigh and Love), etc. In this article, we will consider the possibility of using two types of waves for road surface diagnostics – compressional and flexural standing waves.

Compressional standing waves

We will limit ourselves to one type of body standing waves (compressional) since in our experiments we recorded only the vertical component of acoustic noise. In a previously published paper (Kolesnikov and Fedin, 2018), we proposed a passive seismic method for detecting underground voids, which is based on extracting vertical compressional standing waves from the noise field. Compressional standing waves can form under the influence of microseisms in the space between the earth's surface and the sharp boundary nearest to it. With regard to engineering seismic problems, such a boundary could be, for example, the upper surface of the cavity or the boundary of near-surface unconsolidated soils with underlying bedrocks (the lower boundary of the near-surface low-velocity layer).

As shown by physical modelling (Kolesnikov and Fedin, 2018) and field experiments (Fedin *et al.*, 2021), such waves can be extracted by accumulating a large number of amplitude spectra from noise records. The spectra accumulation leads to the appearance of regular peaks on the averaged spectrum, which correspond to standing waves. The criterion for detecting these standing waves is the regularity of their peaks.

Physically, this follows from the fact that nodes are formed at the boundary of the near-surface layer with an acoustically more rigid medium (a medium with a higher acoustic impedance), and antinodes of standing waves are formed at the boundary with an acoustically less rigid medium (including at the free boundary). Therefore, depending on the boundary conditions, either an integer number of half-lengths or an odd number of quarter-lengths of standing waves is placed between the layer boundaries. The distribution of the amplitudes of the first three modes of compressional standing waves in the near-surface layer with an acoustically less rigid medium (or with a cavity) and with an acoustically more rigid medium border below it is schematically shown in Figure 1.

According to the formation mechanism, compressional standing waves in the layer with two free or one free and one fixed boundaries are similar to extensional standing waves in thin rods that are not fixed or fixed only at one end (Khaykin, 1971). In both cases, standing waves are formed as a result of interference of compressional or extensional waves reflected either without phase change (from the fixed boundary layer or fixed end of the rod, where the nodes of standing waves are formed) or with phase inversion (from free boundaries of the layer or loose ends of the rod, antinodes appear here).

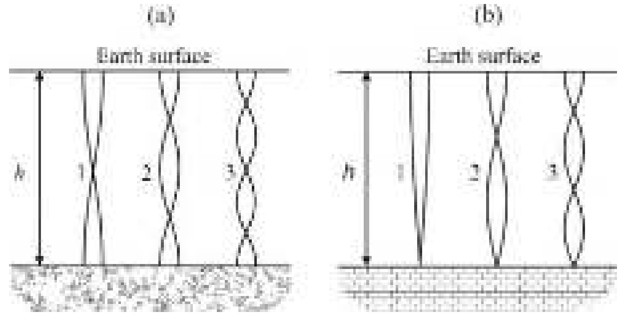

Figure 1 Distribution of the amplitudes of the first three modes of compressional standing waves in the near-surface layer: (a) with an acoustically less rigid base (or with a cavity) and (b) with an acoustically more rigid base below it.

The frequencies of compressional standing waves in the near-surface layer (natural frequencies of the layer) are determined by the following equations (Kramer, 1996; Pain, 2005):

$$f_n = \frac{nV_p}{2h}\ , \tag{1}$$

if there is an acoustically less rigid medium (or a cavity) under the layer, or:

$$f_n = \frac{(2n-1)\,V_p}{4h}, \tag{2}$$

if the layer lies on an acoustically more rigid medium. Here $n = 1,2,3,\ldots$ is the mode number of standing waves, V_p is the velocity of longitudinal waves and h is the layer thickness.

In both cases, the interval between adjacent natural frequencies $\Delta f = (f_{n+1} - f_n)$ is equal to $V_p/2h$. Therefore, at a known velocity V_p of the near-surface layer material, the value of Δf can be used to investigate the layer thickness using the following formula:

$$h = \frac{V_p}{2\Delta f}. \tag{3}$$

In addition, if the layer lies on an acoustically more rigid base, then the voids are formed under it will manifest a change in the distribution of the peaks of the standing wave on the frequency axis of the averaged spectra. Above a rigid base, in accordance with formula (2), the frequency of the lowest mode should be equal to $\Delta f/2$ and over cavities, in accordance with formula (1), it should be equal to Δf.

Flexural standing waves

However, in the case of a pavement lying on an acoustically less rigid base, it is obvious that with constant elastic properties and thickness of the pavement, the appearance of a cavity under the asphalt layer will not lead to a change in the frequencies of vertical compressional standing waves. Both above and outside the cavity, reflections from the lower boundary will occur with phase inversion, the antinodes of compressional standing waves will be observed on both the upper and lower boundaries of the pavement and their frequencies can be determined by formula (1). That is to say, in this case, the frequencies of compressional standing waves cannot be used for detecting cavities under the pavement, although, as will be shown below, they may serve as an indicator of changes in the thickness of the pavement and the nature of the underlying layer.

At the same time, if the horizontal dimensions of the cavity under the pavement substantially exceed its thickness, then a part of the pavement above the cavity can be considered as a plate fixed along its perimeter (or its part), in which flexural standing waves can be formed. Waves of this type are formed as a result of the interference of travelling anti-symmetric (flexural) Lamb waves, they are similar to vibrations of membranes fully or partially fixed at the edges. The distribution of nodes and antinodes of flexural standing waves in membranes, even of a relatively simple shape, can have a rather complex appearance (Pain, 2005). Some properties of these waves are also significantly different from the properties of vertical compressional standing waves.

First, the frequencies of these waves should be significantly lower than the frequencies of compressional standing waves due to the lower velocity of the flexural waves and the predominance of the horizontal dimensions of the unfixed part of the plate over the vertical ones. Second, with sufficiently detailed measurements on the plate surface, one can observe the shapes of different modes of flexural standing waves, their nodes and antinodes. Third, quasi-regular peaks associated with flexural standing waves should be located on the frequency axis of the averaged spectra not at an equal distance from each other due to the strong frequency dependence (dispersion) of the velocity of the flexural waves.

Nonetheless, as will be shown below, the indicated properties of flexural standing waves can be used to identify cavities under asphalt pavement and to estimate their sizes. However, we emphasize that this approach is applicable only in cases where the horizontal dimensions of the cavity are noticeably greater than the thickness of the asphalt layer. This is due to the fact that flexural standing waves are formed as a result of interference of anti-symmetric (flexural) Lamb waves, which, with increasing frequency, are gradually transformed into Rayleigh waves propagating along the upper and lower surfaces of the layer (Krautkramer and Krautkramer, 1990). The thicker the cover layer, the lower the frequencies at which such a transformation occurs. At the same time, the frequencies of flexural standing waves depend on the horizontal dimensions of the 'membrane' (the section of the asphalt layer directly above the cavity). The smaller these sizes, the higher the frequencies.

It follows from this that an increase in the ratio of the thickness of the cover layer to the horizontal dimensions of the cavity should lead to a gradual 'attenuation', first of the high-frequency modes of flexural standing waves and then of the modes of lower orders. This ratio determines the minimum horizontal dimensions of cavities that can be detected by the method of flexural standing waves. To determine the 'threshold' values of this ratio, special studies are required, since the frequencies of the standing waves also depend on the cover material. Taking into account the experimental results presented below, it can be assumed that under our conditions the method of flexural standing waves is applicable to the detection of cavities if their horizontal dimensions are at least five to seven times greater than the thickness of the asphalt layer.

THE STUDY OBJECT AND METHOD OF OBSERVATION

To assess the possibility of diagnosing asphalt pavements with elastic standing waves, we carried out experimental work using acoustic noise recording on the sidewalk of Pirogova Street (Fig. 2a) in Akademgorodok – the southern region of Novosibirsk (Russia). The sidewalk has an asphalt concrete pavement (hereinafter – asphalt pavement) with a thickness of 4–5 cm based on the visual assessment. The base of the asphalt pavement is mainly a gravel–sand mixture, and only in some small areas the asphalt is laid on top of the concrete base.

Figure 2(b) shows a cavity formed under the asphalt pavement at one point on the edge of the sidewalk. At this point, detailed areal observations were carried out in order to evaluate the possibilities of detecting cavities under a solid pavement using standing waves. Moreover, on the sidewalk, profile observations at 10 m intervals throughout the street (with a total length of about 1800 m) were carried out. The purpose of these observations was to assess the ability to investigate

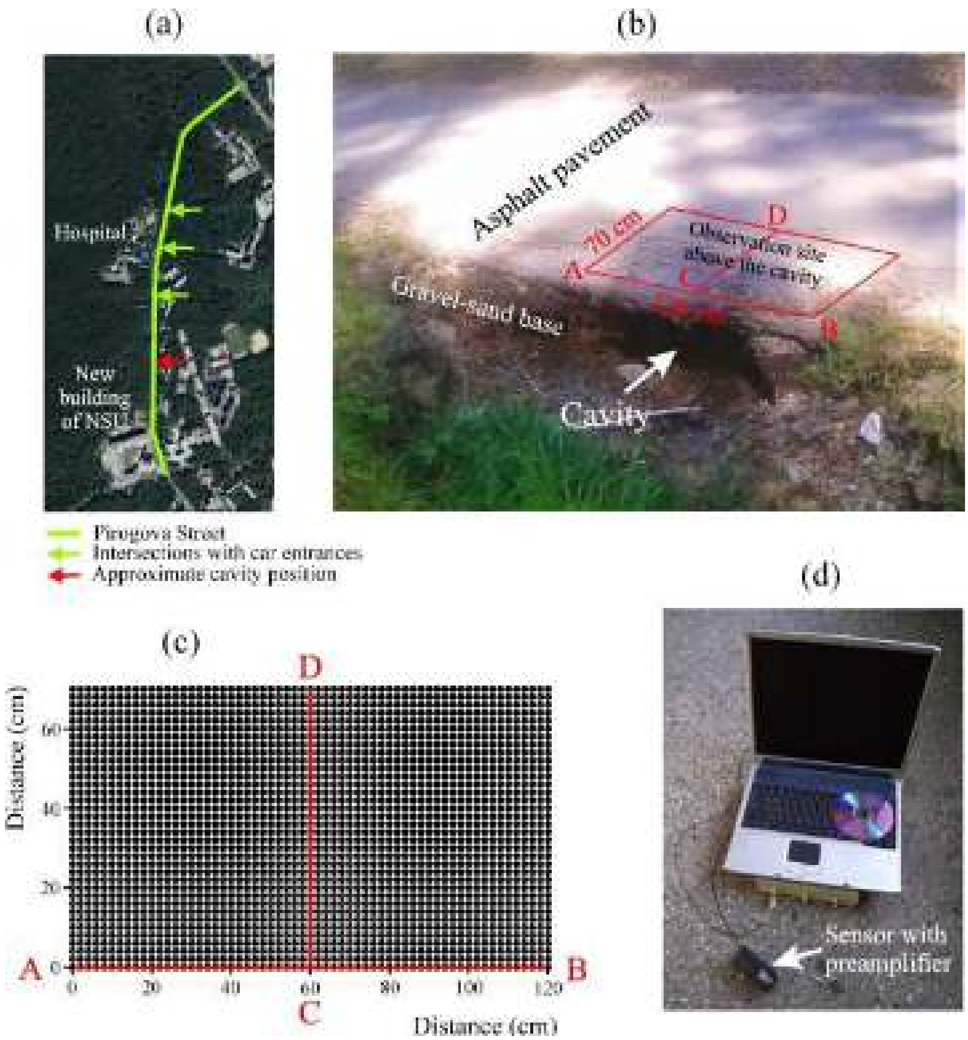

Figure 2 (a) Scheme of the worksite, (b) the position of the areal observational system over the cavity formed under the asphalt pavement, (c) the observation system diagram (observation points are shown in black circles) and (d) measuring equipment.

the thickness of the pavement and the type of underlying base (acoustically harder concrete or less rigid soil).

The dimensions of the cavity, shown in Figure 2(b), were approximately 105 cm along the edge of the sidewalk and 65–70 cm in the widest place in the transverse direction. In this area, measurements were carried out at the nodes of a square network on an area observation system with dimensions of 120 cm in the direction along the sidewalk and 70 cm across it, with a step of 2 cm between adjacent observation points (Fig. 2c). Due to the uneven border of the pavement, no observations were made near its edge (in a band of about 7–10 cm wide). Two perpendicular profiles, shown in Figure. 2(b,c) with red lines, present the relative dimensions of the observation system and the cavity under the asphalt pavement. The data for these profiles were analysed in more detail than for the other points of the area observation system.

According to preliminary assessments, the frequencies of several lower modes of the standing waves studied in this work (flexural and vertical compressional) for objects such as asphalt pavements and cavities under them must be in the range of the few hundreds of hertz to the few hundreds of kilohertz. Therefore, to register noise signals, we used the same equipment that we used in laboratory experiments on physical modelling (Kolesnikov and Fedin, 2018). This equipment (B-423 digital oscilloscope with a 1-MHz sampling frequency and a piston-type broadband piezoceramic sensor, 2 mm in diameter and with a preamplifier) can record signals in such a frequency range (Fig. 2d).

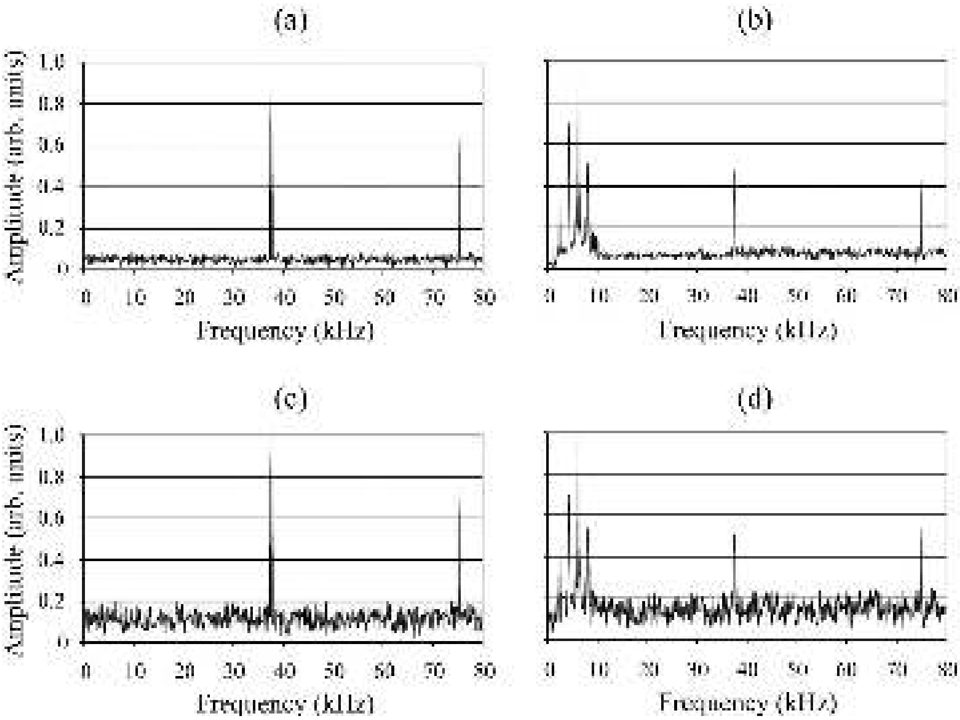

Figure 3 Examples of averaged amplitude spectra of noise records with a duration of 6.5 s obtained with an dynamic noise source (a) away from the cavity and (b) above it; (c) and (d), averaged spectra of "natural" noise recorded at the same points within 20 min.

To reduce the observation time, we generated additional noise in the asphalt pavement using a brush with stiff bristles. Noise impact was performed during measurements near each observation point in its immediate vicinity (at a distance of 10–15 cm). With such an additional source of acoustic noise, the duration of noise records at each point was approximately 6.5 s, which is sufficient for a surefooted separation of standing waves from noise. Note that to achieve a similar effect when recording natural noise, measurements would have to be taken at each point for at least 20 min (Fig. 3).

THE RESULTS OF PROCESSING NOISE DATA OBTAINED OVER THE CAVITY AND NEXT TO IT

During data processing, the noise records were divided into fragments of approximately 33 ms ($2^{15} = 32{,}768$ samples), after which the amplitude spectra of these fragments were accumulated. The examples of averaged (accumulated) amplitude spectra for observation points away from the cavity and above it is shown in Figure 3. As you can see, outside the cavity (Fig. 3a,c), the spectrum has two sharp peaks at frequencies of 37.4 and 74.8 kHz, which is consistent with formula (1).

These peaks correspond to vertical compressional standing waves. At a known velocity V_p of longitudinal waves in asphalt, their frequencies make it possible to estimate the thickness of the asphalt pavement using formula (1). Measurements made by the pulse method on the asphalt pavement gave an approximate value of the velocity $V_p = 3260$ m/s. For such a velocity V_p and the frequency of the lowest standing wave mode ($f_1 = 37.4$ kHz) determined by the averaged spectrum, the thickness of the asphalt layer according to formula (1) is about 4.4 cm, which is consistent with visual assessments of 4.5 cm at this point of the sidewalk.

Over the cavity (Fig. 3b,d), the averaged spectrum is significantly different from away from the cavity (Figure 3a,c). Although it also deonstrates regular peaks corresponding to compressional standing waves, with practically the same frequencies as shown in (Fig. 3a,c) (differences do not exceed 0.5%), additional, quasi-regular peaks appear in the low-frequency part of the spectrum, which as we will show below correspond to flexural standing waves.

Figure 4 shows the averaged amplitude spectra of noise recorded at all points of the two profiles, which are shown in Figure 2(b,c) with red lines. As you can see, the amplitudes of the first and second modes of vertical compressional standing waves along the entire length of the profiles do not have

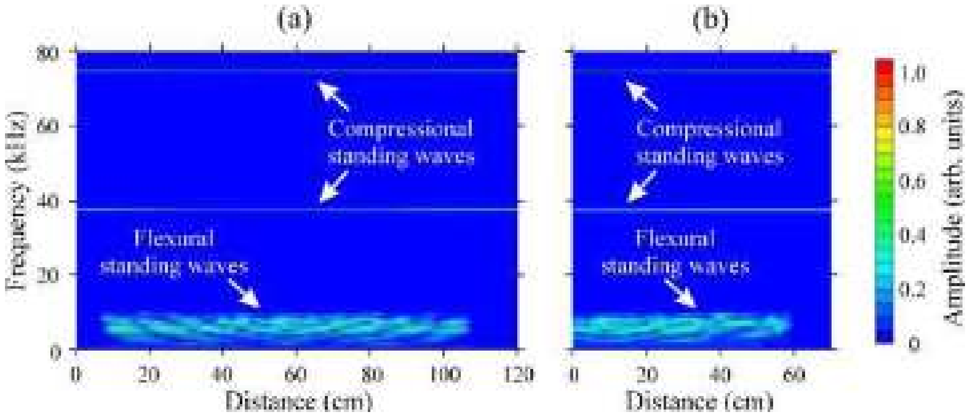

Figure 4 Distribution of averaged amplitude spectra of noise records along the profiles (a) AB and (b) CD.

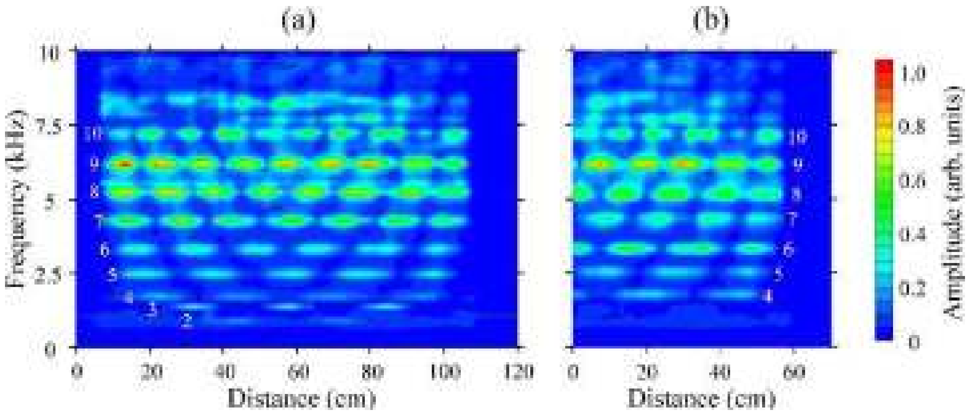

Figure 5 The low-frequency part of the averaged amplitude spectra are shown in Figure 4; the numerals indicate the conditional numbers of the modes of flexural standing waves.

node points, since the measurements were carried out on the earth surface, that is, at the antinodes of all modes of this type of standing waves. At all points of the two profiles, as in Figure 3, the frequency of the second mode is equal to the doubled frequency of the first mode, which is consistent with formula (1), since either at the base of the asphalt pavement there is an acoustically less rigid material or the base is absent (in the cavity area).

At the same time, in the low-frequency part of the spectra above the cavity, there is an alternation of nodes and antinodes for each mode, the number of which increases with an increase in frequency. Such alternation is typical for observations along the profile of standing waves formed in a confined body. This can be seen in detail in Figure 5, where on a larger scale the low-frequency part of the averaged amplitude spectra is represented.

The alternations of nodes and antinodes at quasi-regular frequencies (the same as in AB and CD profiles) in Figure 5 reflect the forms of a family of flexural standing waves, which are formed under the influence of acoustic noise in the non-fixed portion of the asphalt pavement above the cavity. These are exactly flexural waves because their frequencies are significantly lower than the frequencies of vertical compressional standing waves, and outside the cavity there are practically no oscillations at these frequencies. In addition, the interval between the frequencies of adjacent modes of standing waves in the spectra is not constant, which indicates characteristics for flexural waves frequency velocity dispersion.

Numbers in white in Figure 5(a) indicate mode numbers of flexural standing waves. We note that in two-dimensional bodies of the membrane type, especially of an irregular shape, the numbering of standing wave modes can only be conditional because of the variety of possible forms of such waves. This is confirmed by the results of our numerical experiments with the finite element method using the MSC Nastran software (http://www.mscsoftware.com/product/msc-nastran).

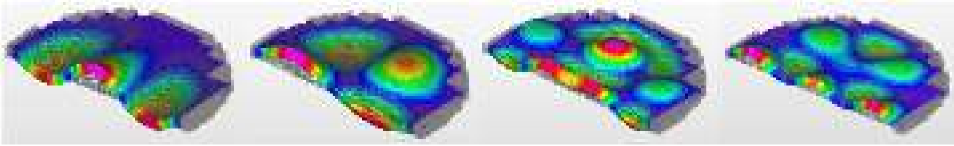

Figure 6 Examples of calculating several forms of flexural oscillations in the numerical model of the pavement above the cavity.

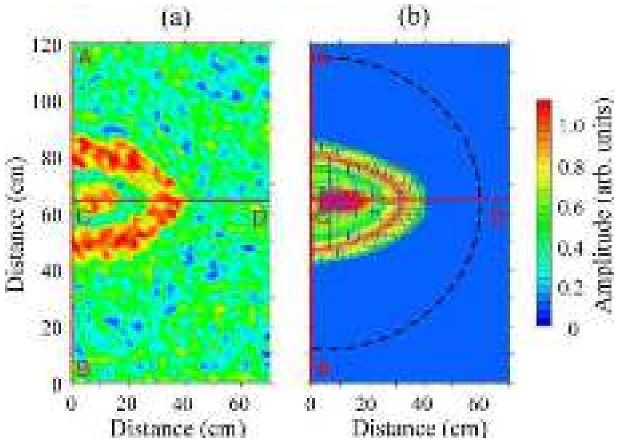

Figure 7 The distribution of the area of observations of the amplitudes of (a) the mode with a frequency of 0.88 kHz (conditional number 2 in Fig. 5) from the experimental data and (b) the mode with a frequency of 0.89 kHz from the results of numerical simulation; the red lines show the position of the AB and CD profiles, dotted line – the position of the cavity boundary in the numerical model.

Some examples of flexural oscillations for the numerical model of the pavement over a cavity, which will be discussed below, are shown in Figure 6. In this study, we used conditional numbering reflecting the number of antinodes of flexural standing waves in the AB profile above the cavity.

The CD transverse profile did not reach the asphalt edge, since it was deformed quite strongly (Fig. 2b). Therefore, it is impossible to determine with certainty the mode numbers by the number of antinodes and nodes in the section of this profile above the cavity. However, judging by the fact that the frequencies of the modes observed in Figure 5(b) almost coincides with the frequencies of the mode numbers 4−10 shown in Figure 5(a), it can be assumed that these are the modes of the same flexural standing waves. This is illustrated in Figure 7(a), which shows the distribution over the observation area of the amplitudes of mode 2 (at a frequency of 0.88 kHz).

For comparison, Figure 7(b) shows the results of computer simulation of this mode by the finite element method. The calculations were carried out using the MSC Nastran software package. The model had the form of a double-layer cube measuring $100 \times 100 \times 100$ m^3. In the upper part of the lower layer imitating the base of the asphalt pavement, there was a hollow (model of a cavity) with a depth of 15 cm with horizontal dimensions approximately corresponding to the dimensions of the cavity shown in Figure 2(b). The horizontal projection of the hollow is shown in Figure 7(b) with a dotted line. A layer with a hollow was overlapped in a layer of constant thickness of 4.5 cm (model of pavement). At the boundary of the layers, excluding the area of the hollow, the conditions of rigid contact were specified. The cubic elements of the calculated grid had a size of 0.15 cm in a $4.5 \times 4.5 \times 4.5$ m^3 region, including the cavity under the upper layer, and 4.5 cm in the rest of the model.

In the calculations, the experimentally determined parameters of the upper asphalt layer were as follows: a density $\rho = 2.43$ g/cm^3 and a velocity of longitudinal waves $V_p =$ 3260 m/s. We did not measure the velocity of the shear waves. In the calculations, it was set at about 0.6 of the velocity of the longitudinal waves, that is $V_s = 1960$ m/s. The parameters of the lower layer practically do not affect the flexural standing waves in the upper layer; they were assumed to be $\rho = 1.75$ g/cm^3, $V_p = 800$ m/s and $V_s = 460$ m/s.

An elastic model was used in the calculations since the pavement of this sidewalk was made of fairly rigid asphalt concrete. This is confirmed by the relatively high-velocity, V_p = 3260 m/s, as well as the high-quality factor of this material (the latter is indicated by very sharp resonance peaks in Fig. 3). In addition, the hardness of the pavement is indicated by the weak temperature dependence of this asphalt concrete, which is uncharacteristic of asphalt with a high content of bituminous materials. For example, repeated measurements were carried out over the same cavity during the winter period and showed an increase in the frequencies of compressional standing waves in the pavement (and, accordingly, the velocity V_p) of only 6.5% with a temperature decrease of more than 30°.

In the computer simulation, the load on the upper surface of the asphalt layer was set in the form of a pressure uniformly distributed over the area with the characteristics of 'white noise'. The calculations were carried out in the frequency range of 0.8−7.5 kHz; as a result, nine modes of flexural oscillations were obtained along with other (low-amplitude) modes. The frequencies of these flexural modes are consistent with determined experimentally modes numbered in Figure 5 – the differences do not exceed 5%. Figure 7(b) shows the distribution of the area of observation of the calculated amplitudes of the mode with a frequency of 0.89 kHz, which is closest to the experimentally determined frequency of 0.88 kHz of the mode noted in Figure 5(a) with a conditional number 2. As follows from Figure 7, the experimentally obtained amplitude distribution of the area of observations at a qualitative level is consistent with the results of numerical simulation.

Thus, a field experiment showed that the appearance of cavities under an asphalt pavement leads to the formation of flexural standing waves under the influence of acoustic noise on its non-fixed portion. The parameters of these waves can be used to detect such cavities and estimate their sizes. However, it should be kept in mind that using only standing modes of low orders is it possible to obtain significantly low estimates of the dimensions of the cavity, which is clearly seen in Figure 7. This is due to the fact that when the mode order decreases, the antinodes shift from the edges of the cavity to their central part (Fig. 5a). For higher order modes, one can get more reliable estimates of the real dimensions of the cavity. For example, the position of the extreme nodes on the profile AB corresponds to the profile points with coordinates approximately 7 cm and 107 cm for modes of flexural standing waves marked with numbers 7–10 in Figure 5(a). For the same modes in Figure 5(b), the rightmost nodes correspond to the coordinate 57 cm. Considering that the measurements were taken at a distance of about 7–10 cm from the edge of the sidewalk, these estimates are in good agreement with direct measurements of the length of the cavity along the edge of the sidewalk (approximately 105 cm) and its transverse dimensions (65–70 cm).

ON THE POSSIBILITY OF INVESTIGATING THE THICKNESS OF AN ASPHALT PAVEMENT AND THE QUALITATIVE ASSESSMENT OF THE ACOUSTIC STIFFNESS OF ITS BASE BY VERTICAL COMPRESSIONAL STANDING WAVES

The parameters of vertical compressional standing waves in the case of an asphalt pavement lying on a softer base are not informative about determined cavities, but they can be used to investigate the thickness of the pavement and the type of its base (underlying layer). To demonstrate this, in addition to measurements in the cavity area, we conducted point measurements of noise along the entire length of the same sidewalk.

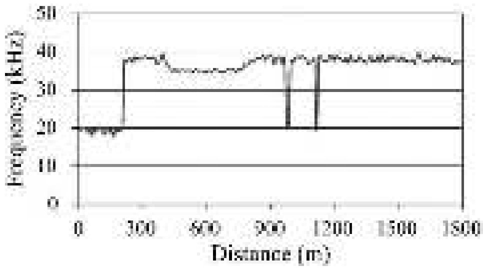

Figure 8 Change of the frequency of the lower (first) mode of compressional standing waves along the sidewalk.

As noted above, the total length of the sidewalk is 1800 m and profile observations on its surface were carried out with spacing of 10 m.

The graph in Figure 8 shows how the frequency of the lowest (first) mode of vertical compressional standing waves changes along the sidewalk, starting from the beginning of the Pirogova Street, near the new building of the Novosibirsk State University, until its completion (Fig. 2a). As you can see, the graph shows both relatively small (up to 10–15%) fluctuations and sharp (approximately two times) changes in the frequency of the lowest mode. Small fluctuations are mainly related to the change in the thickness of the asphalt pavement. The sharp changes are caused by a change in the material of the base, most likely from sand–gravel to concrete and vice versa.

At the interval of 0–210 m, the sidewalk runs along the recently built new building of the Novosibirsk State University. Apparently, during the reconstruction of the sidewalk, it was reinforced with a concrete base under a layer of asphalt. The presence of a concrete base can be assumed in the area at the 980 m and 1120 m marks since here the observation points were located at the intersections of the sidewalk with the car entrances to the territory of the clinical hospital. In Figure 2(a), the intersections of the sidewalk with car entrances are marked by arrows.

A change in the material of the underlying layer from acoustically less rigid to more rigid than the material of the pavement leads to a change in the nature of the distribution of the peaks of standing waves on the frequency axis. If in most of the pavement, this distribution corresponds to formula (1), for example the spectrum shown in Figure 2(a,c); then at places where the underlying layer has a greater acoustic stiffness than the pavement, it corresponds to formula (2). An example of such a spectrum is shown in Figure 9. At the same time, the interval Δf between adjacent natural frequencies as in other parts of the pavement is 35–40 kHz.

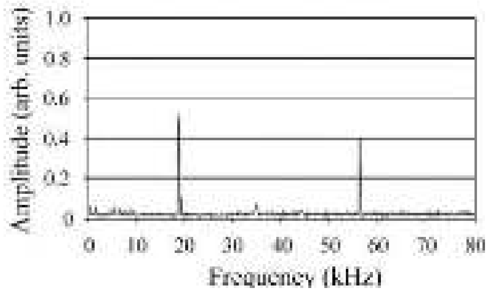

Figure 9 The averaged amplitude spectrum of the noise record obtained at the intersection of the sidewalk with the car entrance to the hospital campus, marked by the upper arrow in Figure 2(a).

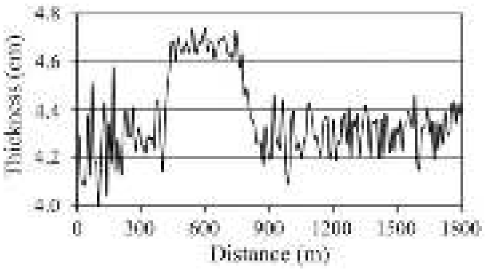

Figure 10 Change of the asphalt layer thickness along the sidewalk.

It is also interesting to note that, at the 760 m mark, the pavement also intersects with another entrance to the hospital campus, but there is no sharp change in the distribution of the peaks of the standing wave at the frequency axis. It can be assumed that at this intersection the asphalt pavement was not reinforced by an underlying concrete base.

Figure 10 shows the change in the thickness of the asphalt layer along the sidewalk, calculated using formula (3) with the experimentally determined velocity of longitudinal waves in asphalt $V_p = 3260$ m/s. The initial data were the frequencies of the lowest mode (Fig. 8). When calculating in accordance with the explanations to formula (3), depending on the distribution of resonant peaks on the frequency axis of the averaged spectra, the interval Δf was taken to be equal to either the frequency f_1 of the lowest mode, if the distribution of peaks correspond to formula (1) or its doubled value if the distribution of peaks correspond to formula (2).

As follows from Figure 10, the thickness of the asphalt layer along the entire length of the sidewalk deviates from the average value (4.37 cm) by no more than 10%. Recall that at the site of the detailed study (Fig. 2b), the measured asphalt thickness is approximately 4.4–4.5 cm, which is consistent with the data shown in Figure 10. This indirectly indicates the effectiveness of using standing waves to investigate the thickness of the asphalt pavement.

In conclusion, we note that, recently at least, for some materials there have been data that possibly may require modifying formula (1) by introducing a correction factor on its right-hand side. The introduction of this factor, according to Gibson and Popovics (2005), can reduce the calculated natural frequencies by several percentages. On the one hand, it is not difficult to introduce a correction factor, but, on the other hand, our computer simulation showed that the frequencies of the compressional standing waves calculated by formula (1) for the model we used differ by no more than 0.1% from those calculated by the finite element method. Approximately, the same differences were obtained when comparing formula (2) with the results of computer simulation, if we replace the lower layer in the model with an acoustically more rigid one than the upper one (in this case, for the lower layer we set $\rho = 2.5$ g/cm^3, $V_p = 6000$ m/s, $V_s = 3600$ m/s). In our case, noticeable differences between the results of computer simulation and the values of frequencies calculated using formulas (1) and (2) were observed only with a significant decrease in the calculated area and/or increase in the elements of the calculated grid.

CONCLUSIONS

The experimental results obtained showed that the standing waves method can be successfully used to detect cavities under a rigid pavement, as well as to investigate its thickness and estimate the ratio of acoustic stiffness of the pavement and the underlying layer. Standing waves can be extracted from the noise field by accumulating a large number of amplitude spectra of noise signals recorded on the pavement.

Although the proposed method in this modification is not very technologically advanced, it can be successfully used for a detailed study of the pavement plots on which periodically cavities of a different nature occur, as well as to refine the results of more productive, but less accurate methods. Moreover, the applicability of the method can be improved by using more powerful artificial sources of both noise and non-noise types, for example sweep signals of vibrators with a quite wide frequency range.

ACKNOWLEDGEMENTS

We are grateful to the mayor's office of the city of Novosibirsk for financial support of this work within the framework of the project 'Development of technology for operational monitoring of the state of engineering structures by jointly using geophysics, physical and numerical modelling methods'.

CONFLICTS OF INTEREST

No potential conflict of interest was reported by the authors.

DATA AVAILABILITY STATEMENT

The data that support the findings of this study are available from the corresponding author, L. Ngomayezwe, upon request.

ORCID

L. Ngomayezwe https://orcid.org/0000-0003-4511-1903

REFERENCES

Al-Qadi, I.L. and Lahouar, S. (2005) Measuring rebar cover depth in rigid pavements with ground-penetrating radar. *Transportation Research Record: Journal of the Transportation Research Board*, 1907(1), 80–85.

Al-Qadi, I.L., Lahouar, S. and Loulizi, A. (2003) Successful application of ground-penetrating radar for quality assurance-quality control of new pavements. *Transportation Research Record: Journal of the Transportation Research Board*, 1861(1), 86–97.

Baker, M.R., Crain, K. and Nazarian, S. (1995) *Determination of pavement thickness with a new ultrasonic device*. Research Report 1966-1. Center for Highway Materials Research, University of Texas, El Paso.

Benedetto, A. and Pensa, S. (2007) Indirect diagnosis of pavement structural damages using surface GPR reflection techniques. *Journal of Applied Geophysics*, 62(2), 107–123.

Cassidy, N.J., Eddies, R. and Dods, S. (2011) Void detection beneath reinforced concrete sections: the practical application of ground-penetrating radar and ultrasonic techniques. *Journal of Applied Geophysics*, 74(4), 263–276.

Celaya, M. and Nazarian, S. (2006) Seismic testing to determine quality of hot-mix asphalt. *Journal of the Transportation Research Board*, 1946, 113–122.

Choi, W.Y. and Park, K.K. (2019) Array type miniaturized ultrasonic sensors to detect urban sinkholes. *Measurement*, 141, 371–379.

Dashevsky, Y.A., Dashevsky, O. Y., Filkovsky, M.I., Synakh, V.S. (2005) Capacitance sounding: A new geophysical method for asphalt pavement quality evaluation. *Journal of Applied Geophysics*, 57(2), 95–106.

Derobert, X., Fauchard, C., Côte, P., Brusq, L., Guillanton, E., Dauvignac, J.Y., and Pichot, Ch. (2001) Step-frequency radar applied on thin road layers. *Journal of Applied Geophysics*, 47(3–4), 317–325.

Fedin, K. V., Kolesnikov, Y. I. and Ngomayezwe, L. (2021) Mapping of underground cavities by the passive seismic standing waves method: The case study of Barsukovskaya cave (Novosibirsk region, Russia). *Geophysical Prospecting*, 69(1), 167–179.

Fedorova, L.L., Savvin, D. V., Mandarov, D. A., Fedorov, M. P. (2017) GPR diagnosis of cryogenic processes in soils of highway subgrade in the city of Yakutsk. *Engineering Survey*, 9, 66–73 (in Russian).

Freeseman, K., Khazanovich, L. and Hoegh, K. (2018) Nondestructive analysis techniques for freeze-thaw damage detection in concrete slabs using shear waves. *International Journal of Pavement Research and Technology*, 11(8), 800–812.

Gibson, A. and Popovics, J.S. (2005) Lamb wave basis for impact-echo method analysis. *Journal of Engineering Mechanics*, 131(4), 438–443.

Hoegh, K., Khazanovich, L., Maser, K. and Tran, N. (2012) Evaluation of ultrasonic technique for detecting delamination in asphalt pavements. *Transportation Research Record: Journal of the Transportation Research Board*, 2306(1), 105–110.

Hoegh, K., Khazanovich, L. and Yu, H.T. (2011) Ultrasonic tomography technique for evaluation of concrete pavements. *Transportation Research Record: Journal of the Transportation Research Board*, 2232(1), 85–94.

Iodice, M., Muggleton, J.M. and Rustighi, E. (2019) Exploiting spectral differences between two acoustic imaging methods for the in situ evaluation of surface-breaking cracks in asphalt. *Applied Acoustics*, 156, 394–403.

Kassem, E., Chowdhury, A., Scullion, T., Masad, E. (2016) Application of ground-penetrating radar in measuring the density of asphalt pavements and its relationship to mechanical properties. *International Journal of Pavement Engineering*, 17(6), 503–516.

Khamzin, A.K., Varnavina, A. V., Torgashov, E. V., Anderson, N. L., and Sneed, L. H. (2017) Utilization of air-launched ground penetrating radar (GPR) for pavement condition assessment. *Construction and Building Materials*, 141, 130–139.

Khaykin, S.E. (1971) *Physical Foundations of Mechanics*, 2nd edition. Moscow: Nauka (in Russian).

Khazanovich, L., Velasquez, R. and Nesvijski, E.G. (2005) Evaluation of top-down cracks in asphalt pavements by using a self-calibrating ultrasonic technique. *Transportation Research Record Journal of the Transportation Research Board*, 1940(1), 63–68.

Kolesnikov, Y.I. and Fedin, K.V. (2018) Detecting underground cavities using microtremor data: Physical modelling and field experiment. *Geophysical Prospecting*, 66(2), 342–353.

Kolesnikov, Y.I., Fedin, K.V. and Ngomayezwe, L. (2019) Direct determination of resonant properties of near-surface sediments using microtremor. *Soil Dynamics and Earthquake Engineering*, 125, 105739.

Kramer, S.L. (1996) *Geotechnical Earthquake Engineering*. Prentice Hall.

Krautkramer, J. and Krautkramer, H. (1990) *Ultrasonic Testing of Materials*, 4th edition. Springer-Verlag.

Kulizhnikov, A.M. (2001) Application of geo radar technologies in the road service. *Exploration and Protection of Mineral Resources*, 3, 32–34 (in Russian).

Li, J., Walubita, L.F., Simate, G.S., Alvarez, A.E. and Liu, W. (2015) Use of ground-penetrating radar for construction monitoring and evaluation of perpetual pavements. *Natural Hazards*, 75(1), 141–161.

Li, M., Anderson, N., Sneed, L. and Torgashov, E. (2016) Condition assessment of concrete pavements using both ground penetrating radar and stress-wave based techniques. *Journal of Applied Geophysics*, 135, 297–308.

Merenda, M., Praticò, F.G., Fedele, R., Carotenuto, R. and Corte, F.G. (2019) A real-time decision platform for the management of structures and infrastructures. *Electronics*, 8, 1180, 1–22.

Nazarian, S., Baker, M.R. and Crain, K. (1993) *Development and Testing of a Seismic Pavement Analyzer*. SHRP Report H-375SHRP. Washington, DC.: National Research Council

Olenchenko, V.V. and Kondrat'ev, V.G. (2017) Geophysical investigations within the deformation section of a mconstructed on a frozen base. *Bulletin of Northeastern State University*, 27, 116–119 (in Russian).

Pain, H.J. (2005) *The Physics of Vibrations and Waves*, 6th edition. Wiley.

Saarenketo, T. and Scullion, T. (2000) Road evaluation with ground penetrating radar. *Journal of Applied Geophysics*, 43(2–4), 119–138.

Salles, L.S., Khazanovich, L. and Balbo, J.T. (2019) Non-destructive evaluation of crack initiation and propagation in continuously reinforced concrete pavements. *Transportation Research Record: Journal of the Transportation Research Board*, 2673(3), 375–385.